

# LBP-HOG DESCRIPTOR BASED ON MATRIX PROJECTION FOR MAMMOGRAM CLASSIFICATION

Zainab Alhakeem

School of Electrical & Electronic Engineering,  
Yonsei University  
Email: zrkhakim@yonsei.ac.kr

Se-In Jang\*

Department of Statistics and Applied Probability,  
National University of Singapore  
Email: sijang@nus.edu.sg

## ABSTRACT

In image based feature descriptor design, an iterative scanning operation (e.g., convolution) is mainly adopted to extract local information of the image pixels. In this paper, we propose a Matrix based Local Binary Pattern (M-LBP) and a Matrix based Histogram of Oriented Gradients (M-HOG) descriptors based on global matrix projection. An integrated form of M-LBP and M-HOG, namely M-LBP-HOG, is subsequently constructed in a single line of matrix formulation. The proposed descriptors are evaluated using a publicly available mammogram database. The results show promising performance in terms of classification accuracy and computational efficiency.

**Index Terms**— Local Descriptor, Matrix Projection, Local Binary Pattern, Histogram of Oriented Gradients, Mammogram Classification

## 1. INTRODUCTION

Breast cancer is the most common and leading cause of cancer death in women [1]. For breast cancer diagnosis, mammography is usually used for early diagnosis. In order to automate the diagnosis process, Computer-Aided Diagnosis (CAD) systems for mammogram classification have been developed [2, 3]. In these CAD systems, texture and shape features play an important role for classification [4]. Local Binary Pattern (LBP) is a popular local descriptor to extract texture information [5]. Histogram of Oriented Gradients (HOG) is also a popular local descriptor to obtain shape information [6]. These descriptors have shown astonishing performance in [5, 6].

Specifically, LBP extracts illumination-invariant image features from computation which locally finds binary patterns [7]. HOG builds geometric, photometric and invariant image features which compute local gradient histogram obtained from various image directions [6]. However, these descriptors are developed using an iterative scanning operation which is a time-consuming process. As a combination

of LBP and HOG features, an LBP-HOG method takes both useful properties and outperforms the utilization of each descriptor solely in [8], [9] and [10]. However, each descriptor should be separately performed to obtain each feature representation.

In order to avoid this scanning operation, in [11], a Difference Matrix Projection (DMP) descriptor was proposed based on a matrix based pixel difference computation and achieved an approximated HOG. However, this DMP partially presented the matrix form due to the absence of forming a matrix based block normalization.

Our motivation for a new feature descriptor consists of the following: 1) The LBP feature extraction with the iterative scanning is time-consuming; 2) A matrix based block normalization is still required to complete the approximated HOG; and 3) A simple combination of LBP and HOG is needed to efficiently extract both useful features.

Accordingly, the main contributions of this work are as follows:

- 1) Matrix formulations of LBP (M-LBP) and HOG (M-HOG) based on global matrix projection;
- 2) A direct integrated formulation of M-LBP and M-HOG in a single step (M-LBP-HOG).

The remainder of the paper is organized as follows: Section 2 includes a brief review of the LBP descriptor and the matrix based pixel difference computation. In Section 3, we propose two image descriptors in matrix formulations. Then we construct an integrated formulation of these two descriptors. Section 4 presents our experiments, observations and evaluations of the proposed method using a public mammogram database. Concluding remarks are given in Section 5.

## 2. PRELIMINARIES

### 2.1. Local Binary Pattern (LBP)

The Local Binary Pattern (LBP) [5] is a simple yet efficient descriptor adopted in various applications (e.g., face and palm print recognitions [12, 13, 14]). The LBP takes an iterative

\*Corresponding Author.

loop using an odd size window (e.g.,  $3 \times 3$  window) for image scanning to describe each central pixel with its local neighborhood pixels ( $P = 8$ ). The LBP can be expressed as:

$$LBP_P = \sum_{i=0}^{P-1} f(d_i)2^i, \quad (1)$$

where  $d_i = s_i - x_c$  is the pixel difference between the neighborhood pixel  $s_i$  and the center pixel  $x_c$  for each direction from  $0^\circ$  to  $315^\circ$ .  $f(\cdot)$  is the thresholding operation given by  $f(x) = \begin{cases} 1, & \text{if } x \geq 0 \\ 0, & \text{if } x < 0 \end{cases}$ .

## 2.2. Matrix based Pixel Difference Computation

In feature descriptors (e.g., LBP and HOG), an essential step is the computation of the pixel difference within each local window. However, the window based technique suffers from the iterative computation for each pixel. In [11], a matrix based pixel difference computation is formulated to globally calculate the pixel differences based on pre-calculated projection matrices:

$$\mathbf{H}_l = \begin{pmatrix} 0 & \mathbf{I} \\ \mathbf{I} & 0 \end{pmatrix} \begin{matrix} N-l \\ l \end{matrix} \in \mathbb{R}^{N \times N}, \quad (2)$$

$$\mathbf{V}_l = \begin{pmatrix} 0 & \mathbf{I} \\ \mathbf{I} & 0 \end{pmatrix} \begin{matrix} M-l \\ l \end{matrix} \in \mathbb{R}^{M \times M},$$

where  $\mathbf{H}_l$  and  $\mathbf{V}_l$  are matrices to horizontally and vertically compute image derivatives respectively.  $\mathbf{I}$  is the identity matrix,  $M$  and  $N$  respectively are the number of rows and columns of the input image  $\mathbf{X} \in \mathbb{R}^{M \times N}$ , and  $l$  indicates a shifting distance between two neighbor pixels.

## 3. A COMPACT LBP-HOG DESCRIPTOR BASED ON MATRIX MULTIPLICATION

First, we propose a Matrix based LBP descriptor (M-LBP). Additionally, we present a complete version of Matrix based HOG descriptor (M-HOG). We then propose a M-LBP-HOG descriptor which easily employs M-LBP and M-HOG in one matrix formulation.

### 3.1. Matrix Based LBP Descriptor

In [5], the LBP computes the pixel differences for each window in eight directions. The proposed Matrix based LBP descriptor (M-LBP) can be formulated as the weighted sum of eight directional difference matrices as follows:

$$f^{LBP}(\mathbf{X}) = \mathbf{Z}^{LBP} = \sum_{i=1}^{P-1} \sigma(\mathbf{D}_i)2^i, \quad (3)$$

where  $\sigma(\cdot)$  is the step function,  $\mathbf{D}_i = \mathbf{S}_i - \mathbf{X}$ , and

$$\begin{aligned} \mathbf{S}_1 &= \mathbf{V}_1^{-1} \mathbf{X} \mathbf{H}_1, & \mathbf{S}_5 &= \mathbf{V}_1 \mathbf{X} \mathbf{H}_1^{-1}, \\ \mathbf{S}_2 &= \mathbf{V}_1^{-1} \mathbf{X}, & \mathbf{S}_6 &= \mathbf{V}_1 \mathbf{X}, \\ \mathbf{S}_3 &= \mathbf{V}_1^{-1} \mathbf{X} \mathbf{H}_1^{-1}, & \mathbf{S}_7 &= \mathbf{V}_1 \mathbf{X} \mathbf{H}_1, \\ \mathbf{S}_4 &= \mathbf{X} \mathbf{H}_1^{-1}, & \mathbf{S}_8 &= \mathbf{X} \mathbf{H}_1, \end{aligned} \quad (4)$$

are shifting matrices for the eight directions using  $\mathbf{V}_l$  and  $\mathbf{H}_l$  at  $l = 1$  in equation (2). Therefore, in equation (3), the weighted sum provides the pixel differences for each matrix in eight directions.

Based on a synthetic binary image, the process of our proposed M-LBP descriptor is illustrated in Fig.1. The shifting matrix  $\mathbf{S}_i$  is the shifting matrix created by the multiplication operation between the pre-calculated projection matrices with the input image. The difference matrix  $\mathbf{D}_i$  is calculated by subtracting the input image  $\mathbf{X}$  from the shifting matrices. The thresholding operation can be easily obtained using a step function. The output M-LBP image is then given by the sum of the thresholded matrices multiplied by the eight binary codes.

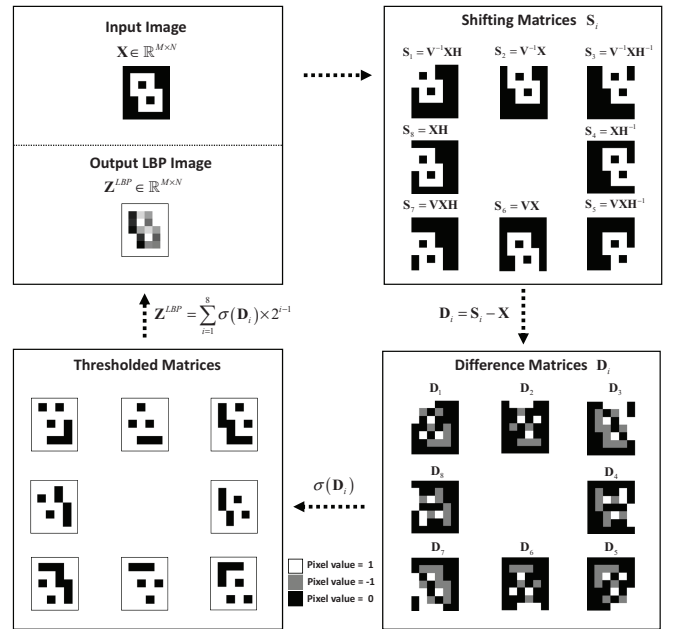


Fig. 1. An overview of the proposed M-LBP descriptor using a synthetic image.

### 3.2. Matrix Based HOG Descriptor

In [11], as an approximated HOG descriptor, a Difference Matrix Projection (DMP) descriptor in matrix form was proposed. The main difference between HOG and DMP is to use the first and the second order gradient information together. This DMP descriptor consists of 1) the matrix based pixel difference computation shown in Section 2.2, 2) a non-overlapping matrix based average pooling and 3) an iterative block normalization which is not in matrix form.

We propose a matrix based block normalization. In addition, an overlapping average pooling operation is also presented to improve the feature representation through the connection between neighbor blocks. The complete Matrix ver-

sion of the HOG can be written as follows:

$$f^{HOG}(\mathbf{X}) = \mathbf{Z}_i^{HOG} = \mathbf{G}_i \circ (\mathbf{L}_{b,v}^T \mathbf{L}_{b,v} \mathbf{G}_i^{\circ 2} \mathbf{R}_{b,v} \mathbf{R}_{b,v}^T)^{\circ(-\frac{1}{2})}, \quad (5)$$

where

$$\mathbf{L}_{c,v} = \begin{bmatrix} \underbrace{1 \dots 1}_{1 \times c} & & & 0 \\ & \underbrace{1 \dots 1}_{1 \times c} & & \\ & & \ddots & \\ 0 & & & \underbrace{1 \dots 1}_{1 \times c} \end{bmatrix} \quad (6)$$

and

$$\mathbf{R}_{c,v} = \begin{bmatrix} \underbrace{1 \dots 1}_{1 \times c} & & & 0 \\ & \underbrace{1 \dots 1}_{1 \times c} & & \\ & & \ddots & \\ 0 & & & \underbrace{1 \dots 1}_{1 \times c} \end{bmatrix}^T \quad (7)$$

are predefined projection matrices which can address overlapping and non-overlapping average pooling. The subscript  $c$  indicates the local desired window size (i.e.,  $2 \times 2$  window at  $c = 2$ ). The subscript  $v$  is an overlapping size between two windows (i.e., non-overlapping at  $v = 0$ ). We denote that  $\circ$  is the Hadamard product. Based on the predefined projection matrices of equation (6) and (7), the combination  $\mathbf{G}_i$  of the non-overlapped average pooling ( $\mathbf{L}_{c_1,0}$  and  $\mathbf{R}_{c_1,0}$ ) and then the overlapped average pooling ( $\mathbf{L}_{c_2,v}$  and  $\mathbf{R}_{c_2,v}$ ) for each cell is given by:

$$\mathbf{G}_i = \mathbf{L}_{c_2,v} \mathbf{F}_i \mathbf{R}_{c_2,v}, \quad i = \{1, 2, \dots, 8\}, \quad (8)$$

where  $\mathbf{F}_i = \mathbf{L}_{c_1,0} (\mathbf{Q}_i - \mathbf{X}) \mathbf{R}_{c_1,0}$ ,

$$\begin{aligned} \mathbf{Q}_1 &= \mathbf{V}_1^{-1} \mathbf{X} \mathbf{H}_1, & \mathbf{Q}_5 &= \mathbf{V}_1^{-2} \mathbf{X} \mathbf{H}_1^2, \\ \mathbf{Q}_2 &= \mathbf{V}_1^{-1} \mathbf{X}, & \mathbf{Q}_6 &= \mathbf{V}_1^{-2} \mathbf{X}, \\ \mathbf{Q}_3 &= \mathbf{V}_1^{-1} \mathbf{X} \mathbf{H}_1^{-1}, & \mathbf{Q}_7 &= \mathbf{V}_1^{-2} \mathbf{X} \mathbf{H}_1^2, \\ \mathbf{Q}_4 &= \mathbf{X} \mathbf{H}_1^{-1}, & \mathbf{Q}_8 &= \mathbf{X} \mathbf{H}_1^{-2}, \end{aligned} \quad (9)$$

and  $\mathbf{Q}_1$  to  $\mathbf{Q}_4$  take the first-order gradients with one pixel distance difference and  $\mathbf{Q}_5$  to  $\mathbf{Q}_8$  include the second-order gradients with two pixel distance difference.  $c_1$  and  $c_2$  are cell sizes for the non-overlapping and overlapping average pooling respectively.

In HOG [6], the  $L_2$ -norm block normalization is defined as  $\frac{\mathbf{g}}{\sqrt{\|\mathbf{g}\|_2^2}}$ , where  $\mathbf{g}$  is a vectorized histogram features in a given block. For the matrix based block normalization with overlapping as seen in equation (5),  $\mathbf{L}_{b,v} \mathbf{G}_i^{\circ 2} \mathbf{R}_{b,v}$  takes the sum of squares  $\|\mathbf{g}\|_2^2$  for each block in a matrix-wise computation. Next, the transposed projection matrices  $\mathbf{L}_{b,v}^T$  and  $\mathbf{R}_{b,v}^T$  is adopted to obtain the same dimension with  $\mathbf{G}_i$  from the down-sampled output of  $\mathbf{L}_{b,v} \mathbf{G}_i^{\circ 2} \mathbf{R}_{b,v}$  due to the overlapping projection matrices  $\mathbf{L}_{b,v}$  and  $\mathbf{R}_{b,v}$ . The superscript  $\circ(-\frac{1}{2})$  is the elementwise inverse of the squared root  $\frac{1}{\sqrt{\cdot}}$ . Then, each block of

$(\mathbf{L}_{b,v}^T \mathbf{L}_{b,v} \mathbf{G}_i^{\circ 2} \mathbf{R}_{b,v} \mathbf{R}_{b,v}^T)^{\circ(-\frac{1}{2})}$  indicates  $\frac{1}{\sqrt{\|\mathbf{g}\|_2^2}}$ , and each block of  $\mathbf{G}_i$  is same with  $\mathbf{g}$ . By the Hadamard product between them, the matrix based block normalization is achieved in global matrix projection.

### 3.3. A Compact LBP-HOG Descriptor

Based on the proposed M-LBP and M-HOG, the proposed M-LBP-HOG in matrix form can be directly and simply written as follows:

$$f_{HOG}^{LBP}(\mathbf{X}) = \mathbf{Z}_i^{LBP} = f^{HOG}(f^{LBP}(\mathbf{X})). \quad (10)$$

For the final M-LBP-HOG features, all  $\mathbf{Z}_i^{LBP}$  are concatenated together into one feature vector.

## 4. EXPERIMENTS

In this section, we evaluate the proposed descriptor for mammogram classification. The experimental goals are as follows: 1) Observing the effect of overlapping pooling among HOG, DMP and the proposed M-HOG; 2) Performance comparison of the proposed M-LBP-HOG with state-of-the-arts methods.

### 4.1. Database and Experimental Setup

The most commonly used database in mammography is the Digital Database of Screening Mammography (DDSM) [15]. Recently, in [16], a Curated Breast Imaging Subset of the DDSM (CBIS-DDSM) has been released with a standardized evaluation. In this experiment, we used the CBIS-DDSM database. The database includes 3,568 ROI images which are categorized into two classes (malignant, benign) for 6,671 patients and the images are resized to a  $56 \times 56$  resolution. By following the data split setting in [16], a training set (2,864 images) and a test set (704 images) are obtained.

For state-of-the-art descriptors, the original LBP [5], HOG [6] and DMP [11] are implemented for comparison. The LBP-HOG is also implemented based on a cascade of the LBP image and the HOG feature representation. For a state-of-the-art mammogram classification system, VGGNet [17] is also implemented. For the parameter settings of each descriptor, we followed the general settings [5], [6], [11] for LBP, HOG, DMP, LBP-HOG, and for the proposed M-LBP, M-HOG and M-LBP-HOG:  $P = 8$ ,  $c_1 \in \{2, 4, 6\}$ ,  $c_2 \in \{2, 4, 6\}$ ,  $v \in \frac{c_2}{2}$  and  $b \in \{2, 4, 6\}$ . The histogram bin sizes of LBP and HOG are respectively fixed at 59 and 9. The LSE and SVM classifiers are utilized with a radial basis function (RBF). The regularization parameter  $\lambda$  of the LSE is fixed at 0.0001. According to [17], the parameters settings of the VGGNet is set.

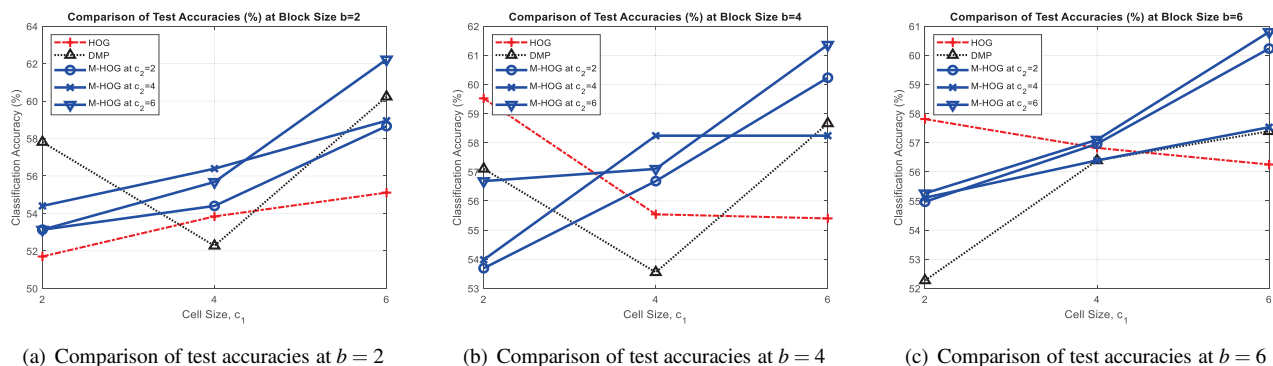


**Fig. 2.** Comparison of HOG, DMP and M-HOG in terms of classification test accuracies (%) on CBIS-DDSM database.

**Table 1.** Comparison of Classification Test Accuracies (%)

Method	LBP	HOG	DMP	LBP-HOG	M-LBP-HOG
VGGNet				63.35	
SVM	60.79	60.80	60.51	63.49	62.36
LSE	56.25	59.52	60.23	62.07	<b>64.35</b>

**Table 2.** Comparison of CPU Processing Time in Seconds

Method	Feature Dimension	Feature Extraction Time	Training Time	Test Time
VGGNet	150,528	-	174,460	209.88
LBP	19,116	53.53	24.40	0.0069
HOG	10,404	42.50	14.59	0.0038
DMP	9,248	62.00	12.97	0.0034
LBP-HOG	10,404	43.21	14.25	0.0038
M-LBP-HOG	1,800	31.13	04.00	0.0008

#### 4.2. Observing the effect of the proposed overlapping pooling among the HOG based descriptors

In order to observe the effect of the proposed M-HOG descriptor compared to the HOG and DMP descriptors, classification test accuracies were acquired at different non-overlapping cell size  $c_1$  and block size  $b$ . Fig. 2 shows the accuracy trends of the proposed overlapping pooling of the M-HOG at different overlapping sizes  $v = \frac{c_2}{c_1}$  in accordance with the different cell sizes  $c_2$ , while  $c_1$  and  $b$  are fixed. The accuracy performances are observed according to the increment of the non-overlapping pooling size  $c_1$ . According to the increment, the performance of the M-HOG is increasing while that of HOG and DMP are unstable. The proposed M-HOG outperformed the other state-of-the-art methods when  $c_1$  is 4 and 6. The best performance is observed in M-HOG where the overlapping pooling is included.

#### 4.3. Performance Comparison and Summary

In terms of classification performance, Table 1 shows the classification accuracies for the compared descriptors, namely LBP, HOG, DMP, LBP-HOG and the proposed M-LBP-HOG. The proposed M-LBP-HOG based on the LSE classifier showed the **best performance** compared to the state-of-the-arts while LBP-HOG based on the SVM classifier and the VGGNet respectively showed the second and the third bests.

In terms of computational performance, Table 2 shows the CPU processing time in seconds. The averaged CPU times are reported over 10 runs. The proposed M-LBP-HOG based on

the LSE classifier showed the best CPU times in the training and test phases due to the predefined projection matrices under global computation form. In addition, the M-LBP-HOG produced the smallest feature dimension which is 5 times less than the other descriptors.

As a summary, we have shown that

- 1) The effectiveness of the overlapping pooling step in the proposed M-HOG compared with HOG and DMP.
- 2) In terms of classification accuracy, the proposed M-LBP-HOG with the LSE classifier achieved better performance with the smallest feature dimension than that of the other state-of-the-art methods.
- 3) In terms of CPU time, the proposed M-LBP-HOG achieved better performance than that of the other state-of-the-art methods due to the efficient computation using the global matrix multiplication.

## 5. CONCLUSION

Different from the iterative scanning based LBP and HOG, we have presented the matrix based LBP (M-LBP) and HOG (M-HOG) using the matrix based pixel difference computation. In addition, the overlapping pooling in matrix form is also presented. The integrated form of the proposed M-LBP and M-HOG descriptors, namely M-LBP-HOG, was then proposed in a matrix formulation. The proposed descriptors were evaluated using the CBIS-DDSM database for mammogram classification where the results show promising performance comparing with state-of-the-art descriptors.

## Acknowledgment

The authors are thankful to Prof. Hong-Goo Kang for his constructive comments and enormous support.

## 6. REFERENCES

- [1] Freddie Bray, Jacques Ferlay, Isabelle Soerjomataram, Rebecca L. Siegel, Lindsey A. Torre, and Ahmedin Jemal, "Global cancer statistics 2018: Globocan estimates

- of incidence and mortality worldwide for 36 cancers in 185 countries,” *CA: A Cancer Journal For Clinicians*, vol. 68, no. 6, pp. 394–424, 2018.
- [2] Arnau Oliver, Xavier Lladó, Robert Martí, Jordi Freixenet, and Reyer Zwiggelaar, “Classifying mammograms using texture information,” in *Medical Image Understanding and Analysis*. Citeseer, 2007, vol. 223.
- [3] Aditya A. Shastri, Deepti Tamrakar, and Kapil Ahuja, “Density-wise two stage mammogram classification using texture exploiting descriptors,” *Expert Systems with Applications*, vol. 99, pp. 71–82, 2018.
- [4] Hamid Soltanian-Zadeh, Siamak Pourabdollah-Nezhad, and Farshid Rafiee Rad, “Shape-based and texture-based feature extraction for classification of microcalcifications in mammograms,” in *Medical Imaging: Image Processing*. International Society for Optics and Photonics, 2001, vol. 4322, pp. 301–311.
- [5] Timo Ojala, Matti Pietikainen, and David Harwood, “Performance evaluation of texture measures with classification based on kullback discrimination of distributions,” in *International Conference on Pattern Recognition (ICPR)*. IEEE, 1994, vol. 1, pp. 582–585.
- [6] Navneet Dalal and Bill Triggs, “Histograms of oriented gradients for human detection,” in *IEEE Conference on Computer Vision and Pattern Recognition (CVPR)*. IEEE, 2005, vol. 1, pp. 886–893.
- [7] Li Liu, Paul Fieguth, Yulan Guo, Xiaogang Wang, and Matti Pietikäinen, “Local binary features for texture classification: Taxonomy and experimental study,” *Pattern Recognition*, vol. 62, pp. 135–160, 2017.
- [8] Xiaoyu Wang, Tony X Han, and Shuicheng Yan, “An hog-lbp human detector with partial occlusion handling,” in *2009 IEEE 12th international conference on computer vision*. IEEE, 2009, pp. 32–39.
- [9] Dimitrios Konstantinidis, Tania Stathaki, Vasileios Argyriou, and Nikolaos Grammalidis, “Building detection using enhanced hog–lbp features and region refinement processes,” *IEEE Journal of Selected Topics in Applied Earth Observations and Remote Sensing*, vol. 10, no. 3, pp. 888–905, 2016.
- [10] Junge Zhang, Kaiqi Huang, Yinan Yu, Tieniu Tan, et al., “Boosted local structured hog-lbp for object localization,” 2011.
- [11] Xing Liu, Kar-Ann Toh, and Jan P Allebach, “Pedestrian detection using pixel difference matrix projection,” *IEEE Transactions on Intelligent Transportation Systems*, 2019.
- [12] Timo Ahonen, Abdenour Hadid, and Matti Pietikainen, “Face description with local binary patterns: Application to face recognition,” *IEEE Transactions on Pattern Analysis and Machine Intelligence*, vol. 28, no. 12, pp. 2037–2041, 2006.
- [13] Alireza Sepas-Moghaddam, Paulo Lobato Correia, and Fernando Pereira, “Light field local binary patterns description for face recognition,” in *IEEE International Conference on Image Processing (ICIP)*. IEEE, 2017, pp. 3815–3819.
- [14] Yufei Han, Zhenan Sun, and Tieniu Tan, “Palmprint recognition using coarse-to-fine statistical image representation,” in *IEEE International Conference on Image Processing (ICIP)*. IEEE, 2009, pp. 1969–1972.
- [15] Michael Heath, Kevin Bowyer, Daniel Kopans, Richard Moore, and W. Philip Kegelmeyer, “The digital database for screening mammography,” in *International Workshop on Digital Mammography*. Medical Physics Publishing, 2000, pp. 212–218.
- [16] Rebecca Sawyer Lee, Francisco Gimenez, Assaf Hoogi, Kanae Kawai Miyake, Mia Gorovoy, and Daniel L. Rubin, “A curated mammography data set for use in computer-aided detection and diagnosis research,” *Scientific Data*, vol. 4, pp. 170–177, 2017.
- [17] Pengcheng Xi, Chang Shu, and Rafik Goubran, “Abnormality detection in mammography using deep convolutional neural networks,” in *IEEE International Symposium on Medical Measurements and Applications (MeMeA)*. IEEE, 2018.
- [18] Felix Juefei-Xu, Vishnu Naresh Boddeti, and Marios Savvides, “Local binary convolutional neural networks,” in *IEEE Conference on Computer Vision and Pattern Recognition (CVPR)*. IEEE, 2017, vol. 1.